WORLD CONFERENCE ON TIMBER ENGINEERING 2025
BRISBANE, AUSTRALIA
Advancing Timber for the Future Built Environment

SEISMIC PERFORMANCE AND NONLINEAR MODEL OF MASS TIMBER BUCKLING RESTRAINED BRACED FRAME

Emily Williamson[1], Chris P. Pantelides[2], Hans-Erik Blomgren [3], Douglas Rammer [4]

ABSTRACT: A timber frame with mass ply lam (MPL) beams and columns and a timber buckling restrained brace (TBRB) was subjected to cyclic loads according to the AISC qualification procedure for conventional buckling restrained braces (BRB). The TBRBs met the requirements for qualification of conventional BRBs; the steel core reached a maximum strain of 3.1% in both tension and compression and the braced frame reached a maximum drift ratio of 4.5%. A numerical OpenSees model of a single-story timber frame with a TBRB was built and validated by TBRB component tests and MPL beam-column joint tests with slotted-in steel plates and steel dowels. The single-story TBRB braced frame model was expanded to an eight-story frame and analyzed using static, cyclic, and earthquake loads. During the simulation of eleven design-level earthquake ground motions, the building experienced a peak inter-story drift at of 2.54% at the first-floor level and a peak floor acceleration of 1.7g at the roof. The numerical model developed in this research of a timber buckling restrained braced frame with TBRBs is novel and could be used to design timber buckling restrained braced frames as a ductile lateral force resisting solution for mass timber buildings in seismic regions.

KEYWORDS: buckling restrained brace, earthquake, lateral force, numerical model, timber

1 – INTRODUCTION

Research has focused on developing new timber lateral force resisting systems to construct resilient buildings in seismic regions. The new systems include rocking cross laminated timber (CLT) shear walls, hybrid timber-steel braced frames, and slip friction joints within CLT shear walls and at the ends of braces. Design principles similar to those for conventional BRBs were used to build and test TBRBs for which the restraining element is constructed with MPP blocks bolted together [1]. A series of component tests with TBRBs was carried out using glulam as the restraining element with steel bearing plates and steel reinforcing plates [2]. Cyclic tests of timber beam-column connections with steel dowels have been carried out [3], followed by a series of single-story TBRB braced frame tests which showed that it achieved 2.8% story drift before TBRB failure [4]. An additional series of TBRBF tests were completed in which some of the TBRBs were enhanced by providing a carbon fiber reinforced polymer (CFRP) wrap at each end of the TBRB casing to provide additional tensile strength to the casing in the perpendicular to grain direction [5]. The subassembly tests of the TBRB frame using TBRBs enhanced with a CFRP wrap were able to achieve 4.5% story drift ratio, and the failure mode of the TBRB was changed to fracture of the steel yielding core although some damage to the MPP casing still occurred during these tests.

OpenSees [6], an open-source research-grade software developed for simulating the structural response to general loads including earthquakes, is used in this study to model the seismic performance of TBRB frames. This software has been used to simulate the cyclic performance of a timber frame with conventional BRBs [7]. OpenSees has also been used to model the behavior of timber-steel dowel connections [3] and conventional BRB components [8]. OpenSees has been used to carry out non-linear time-history analysis of tall timber buildings ([9], [10]). A computational model for a TBRB frame has been developed using design-grade software [11].

The feasibility of the TBRB frame is investigated as a ductile solution by: (i) experiments of a single story

[1] Res. Assist., Dept. of Civil and Env. Eng., Univ. of Utah, USA, emily.diedrich@utah.edu,

[2] Prof., Dept. of Civil and Env. Eng., Univ. of Utah, USA, c.pantelides@utah.edu, https://orcid.org/0000-0003-3309-3488

[3] Struct. Eng., Timberlab, USA, hanserik.blomgren@timberlab.com

[4] Res. Eng., Forest Products Laboratory, USA, douglas.r.rammer@usda.gov

https://doi.org/10.52202/080513-0348

TBRB frame and (ii) a model of a single-story TBRB frame developed in OpenSees. The single-story model was expanded to a model of an eight-story TBRB frame subjected to static, cyclic, and earthquake loads.

2 – PERFORMANCE OF TBRB BRACED FRAME

The experimental timber frame had a story height of 2.29 m and column spacing of 3.05 m with a single diagonal TBRB designed to have an axial yield strength of 178 kN (Figure 1). In cyclic tests, the TBRB frame achieved an interstory drift ratio from 3.1% to 4.5% [4,5]. The TBRB exceeded a cumulative inelastic deformation of 200 which is required for conventional BRB qualification and a strain of 3.1% or 20 times the yield strain of the steel core before tensile fracture.

3 – SINGLE STORY TBRB BRACED FRAME MODEL

A component model of a TBRB was first developed and validated with experimental results [1] before it was incorporated into the single-story model; it consists of two nodes connected by a corotational truss element, as shown in Figure 2, with three materials to simulate hysteretic behaviour: *Steel02*, *Pinching4*, and *Fatigue Material*. More details of the parameters used to construct the model can be found elsewhere [12]. The results from the component model including the hysteresis (Figure 2(b)) and the cumulative hysteretic energy (Figure 2(c)) agree with the experimental results in a satisfactory manner.

The beam-column connections are modelled as 2-node zero-length links with material properties defined for the horizontal, vertical, and rotational directions (Figure 3); the moment-rotation relationship is modelled with the *pinching4* material and is defined by the envelope of the experimental results [3]. A zero-length spring element, with very low stiffness within a range of 3.0 mm and a high stiffness beyond that displacement was used to incorporate the slip of the connections caused by oversized holes in the MPL and steel connecting plates. To determine the force-displacement relationship of the connection in the horizontal and vertical directions, a single-dowel test was completed. The shape of the dowel indicated that the connection had a yield mode IV behaviour and provided a ductile connection; the force-displacement relationship observed during this test was extrapolated to represent each thirty-dowel connection in the timber frame; the total force was obtained by multiplying the single dowel force by the number of dowels included in each connection in the experimental timber frame construction and a group action factor [3].

The performance of the horizontal and vertical components of the connection, including the cyclic degradation, was modelled with the *pinching4* material with the same hysteretic characteristics that were used for the moment-rotation relationship.

A comparison of the experimental results and the numerical model is presented in Figure 4 for the hysteresis curves and the cumulative hysteretic energy, for test I-BRB1 [4]. The model predicts failure of the TBRB which occurred after completion of three cycles at 3.0% story drift ratio; this is one cycle more than the experimental timber frame, which experienced TBRB failure when the MPP casing split apart (Figure 4).

The performance of the TBRB as a whole is captured by combining the *pinching4* and *steel02* materials in parallel and defining strain limits of the TBRB based on those observed during the experimental frame tests in Figure 4. The model slightly overestimates the hysteretic energy dissipation primarily because the experimental timber frames were not able to achieve the full displacement defined in the loading protocol due to slack in the loading application assembly which caused the actual achieved displacement to be slightly less than the defined desired displacement. However, the model accurately captures the loading and unloading stiffness of the system, as well as the slip that occurs within the system when the loading is reversed. Based on these results, the modeling approach was determined to be validated and capable of accurately representing the performance of the TBRB subassembly because it was able to predict the cumulative hysteretic energy within 12% of the experimental results and the maximum force of the model was within 10% of the experimental results. After validating the single-story TBRBF tests, the modeling approach was used to develop a model for an eight-story timber building with TBRB frames, which was used to perform a series of earthquake simulations.

4 – EIGHT-STORY BUILDING TBRB BRACED FRAME MODEL

After validating the single-story TBRB frame tests, the modeling approach was used to develop a model for an eight-story timber building, representing an office building in Los Angeles. It is a four-bay by five-bay building with a column grid spacing of 4.57 m and a story height of 3.35 m, as shown in Figure 5(a). The beams and columns were 381 x 389 mm made with F16 MPL with an elastic modulus equal to 11 GPa [13].

https://doi.org/10.52202/080513-0348

The building was designed using the Equivalent Lateral Force (ELF) procedure defined in ASCE 7-16 for conventional steel concrete BRB systems [14]; the design values used for this building are summarized elsewhere [12]. TBRBFs were selected as the lateral system in both directions of the building. Although the response modification factor (R), for conventional steel-concrete BRB frames is 8.0, an R factor of 3.5 was conservatively selected for this TBRB frame model based on the displacement ductility of the single-story experimental frame. Based on the results of the ELF procedure, it was determined that six TBRBFs were required in the longitudinal direction of the building; moreover, the braces were sized such that the first six stories had TBRBs with 800 kN yield strength and stories seven and eight had TBRBs with 356 kN yield strength.

One of the TBRB frames of the building was modeled as a two-dimensional model for this study. Figure 5(b) shows an elevation of the OpenSees TBRB frame model created for the numerical simulation. One bay of the model is representative of a single TBRBF in the line; the frame was assumed to be pinned to the foundation. In addition to the TBRBF, a leaning column bay was modeled with pinned connections to accurately represent the gravity loads and corresponding P-delta effects by applying the mass which is tributary to the modeled TBRBF at each level. The same beam, column, and TBRB elements from the single-story TBRB frame model were used to create the eight-story TBRB frame model, although the steel core areas of the TBRBs were updated to reflect the steel core areas required for the desired yield strength at various floors.

Gravity loads were applied to the columns at each floor based on tributary area. For the columns in the TBRBF, the gravity load tributary to the column was applied, and for the leaning column, the remaining gravity load in the building tributary to the frame was applied. A live load of 2.9 kPa was applied to the frame as required for office buildings with partitions [14]. The lateral loads applied to the building included static pushover, cyclic loads, and existing earthquake records. The static pushover and cyclic loads were applied as an inverted triangle until a decrease in load occurred. The earthquake loads were applied at the base of the building in the form of acceleration time histories from the PEER Ground Motion Database [15]. Eleven ground motions were selected from the data base, and the spectral accelerations were matched to the target design spectrum for the earthquake with a 10.0% probability of exceedance in 50 years [14] of the building through a multistep matching process in SeismoMatch [16]. Figure 6 shows the selected ground motions and the spectral accelerations, respectively. The model used a Rayleigh damping ratio of 5.0% for the dynamic simulations. An eigenvalue analysis was performed to ensure 95% mass participation. The first three mode have natural periods of 1.21 s, 0.38 s, and 0.21 s with 75.2, 16.7, and 4.7 percent mass participation, respectively.

5 – NUMERICAL RESULTS FOR EIGHT-STORY BUILDING TBRB BRACED FRAME

Eleven different earthquake simulations were run for the eight-story TBRBF, which is part of a six-frame lateral force resisting system in the longer direction of the building. The base shear and roof displacement from the earthquake simulations were compared to the results of the static pushover simulations as shown in Figure 7. The story drift and forces observed as the results of the dynamic simulations are intended to represent the potential demands on the TBRBF during a seismic event; thus, it is expected that the demands are less than the capacity envelope determined by the pushover and cyclic simulations. The maximum roof displacement for all eleven motions remained below the maximum roof displacement of the pushover simulations and the TBRBs in all floors remained intact.

The maximum inter-story drift ratio, residual inter-story drift ratio, and building profile at the peak roof displacement are shown in Figure 8(a,b,c). The inter-story drift ratios and peak displacements were comparable to the pushover simulations. According to the Hazus Earthquake Model Technical Manual [17], the inter-story drift ratio associated with extensive damage to the building is 4.0% for commercial wood-construction buildings with an area greater than 465 m^2. The peak inter-story drift ratio occurred at the first story and was approximately 2.54% during the San Fernando 1971 motion PEL180; this implies that the non-structural components in this building might experience damage, but the structure will not collapse. The single-story experimental timber frame used to calibrate the single-story model achieves less than 3.0% story drift ratio before TBRB failure [4]. However, a subsequent series of cyclic tests showed that the TBRBF has the capacity to reach 4.5% story drift ratio when the ends of the MPP casing were reinforced with a CFRP wrap to provide additional tensile strength in the perpendicular to grain direction [5]. Therefore, an inter-story drift ratio of 2.54% is a reasonable response from the TBRBF which is able to accommodate 4.5% story drift ratio.

The Hazus Earthquake Model Technical Manual [17] defines benchmarks for peak floor acceleration according

to the level of damage to non-structural components. Following the earthquake simulation of the eight-story building TBRB braced frame, the peak floor accelerations were plotted for each motion, as shown in Figure 8(d). The maximum acceleration of 1.7g occurred at the roof for the Imperial Valley 1979 (DLT352), Landers 1992 (YER360), and Northern Calif-03 1954 (FRN314) motions; this level of acceleration is typically associated with damage to the non-structural components. Shake table tests on a six-story light-frame wood building [18] and a two-story mass timber building with rocking CLT shear walls as the LFRS [19] have shown that floor accelerations in this range are acceptable.

6 – CONCLUSION

A numerical model of a single-story timber braced frame with a TBRB was developed using OpenSees which was validated with experimental results. The elements used in the single-story model were used for a TBRB frame which was designed to be part of an eight-story office building located in Los Angeles. The two-dimensional model of the eight-story TBRB frame was subjected to pushover, cyclic and earthquake loads. Based on seismic simulations using eleven ground motions scaled to the target design spectrum for an earthquake with 10.0% probability of exceedance in 50 years the following conclusions can be made:

* The numerical model of the single-story timber frame with a TBRB was able to accurately reproduce the loading and unloading stiffness and cumulative hysteretic energy/ This model, which included the effects of low-cycle fatigue of the steel core, predicted failure of the TBRB within one cycle of the experiment.

* The pushover and cyclic loads applied to the eight-story timber building model resulted in an asymmetric envelope for the TBRBF. This reflects the performance observed during the single-story experimental results in which the TBRB consistently failed in compression after achieving significant ductility.

* In the earthquake simulations of a TBRBF of an eight-story office timber building none of the TBRBs failed. This suggests that the TBRBF system can provide the stiffness, strength and ductility required to resist a design-level seismic event.

* A maximum inter-story drift ratio of 2.54% and maximum roof acceleration of 1.7g that occurred during earthquake simulations are acceptable for this type of building according to performance-based guidelines, and experimental results from cyclic and shake table tests of timber buildings with established lateral force resisting systems.

* Damage to the non-structural components within a timber building at these high levels of drift and acceleration is likely. However, the lateral force resisting system is capable of remaining stable and resilient, as evidenced by the low residual displacements. The structure is likely to remain in service after an earthquake with potentially only some TBRBs requiring replacement.

* The simulation results of the eight-story timber building model show that the TBRB frame is a feasible solution for a ductile timber lateral force resisting system for mass timber buildings. The use of the TBRB in timber buildings is beneficial because it is aesthetically appealing, provides a sustainable solution, and is light-weight and therefore more compatible with the overall weight of a timber building.

* The numerical model developed in this research is based on validation from the experimental results of a series of 2/3-scale TBRB frame quasi static cyclic tests. Further tests of longer TBRBs, with typical dimensions found in actual buildings, should be carried out using quasi-static cyclic loading protocols and full-scale shake table tests to support the numerical simulations.

7 – REFERENCES

[1] C. Murphy, C.P. Pantelides, H.E. Blomgren, D. Rammer. “Development of timber buckling restrained brace for mass timber-braced frames.” In: Journal of Structural Engineering, (2021), 147(5), 04021050.

[2] T. Takeuchi, Y. Terazawa, S. Komuro, T. Kurata, B. Sitler. “Performance and failure modes of mass timber buckling-restrained braces under cyclic loading.” In: Engineering Structures, (2022), 266, 114462.

[3] E. Williamson, C.P. Pantelides, H.E. Blomgren, D. Rammer. “Performance of beam-column connections with mass ply lam and steel dowels under cyclic loads.” In: Journal of Structural Engineering, (2023), 149(6), 04023057.

[4] E. Williamson, C.P. Pantelides, H.E. Blomgren, D. Rammer. “Design and cyclic experiments of a mass timber frame with a timber buckling restrained brace.” In: Journal of Structural Engineering, (2023), 149(10), 04023131.

[5] E. Williamson, C.P. Pantelides, H.E. Blomgren, D. Rammer. “Seismic performance of timber frames with

 https://doi.org/10.52202/080513-0348

timber buckling-restrained braces." In: Journal of Structural Engineering, (2024), 150(6): 04024048.

[6] F. McKenna, M.H. Scott, G.L. Fenves. "Nonlinear finite-element analysis software architecture using object composition." In: Journal of Computing in Civil Engineering, (2010), 24(1): 95-107.

[7] W. Dong, M. Li, C.L. Lee, G. MacRae. "Numerical modelling of glulam frames with buckling restrained braces." In: Engineering Structures, (2021), 239: 112338.

[8] A. Upadhyay, C.P. Pantelides, L. Ibarra. "Residual drift mitigation for bridges retrofitted with buckling restrained braces or self-centering energy dissipation devices." In: Engineering Structures, (2019), 199: 109663.

[9] R. Gohlich, J. Erochko, and J. E. Woods. 2018. "Experimental testing and numerical moment-resisting frame with ductile steel links." In: Earthquake Engineering Structural Dynamics, (2018), 47(6): 1460-1477.

[10] W. Dong, M. Li, T. Sullivan, G. MacRae, C.L. Lee, T. Chang. "Direct displacement-based seismic design of glulam frames with buckling restrained braces." In: Journal of Earthquake Engineering, (2022), 27(8): 2166-2197.

[11] H.E. Blomgren, J.P. Koppitz, A.D. Valdes, E. Ko. "The heavy timber buckling-restrained brace frame as a solution for commercial buildings in regions of high seismicity" In: Proceedings, World Conference on Timber Engineering, (2016), Vienna, Austria.

[12] E. Williamson, C.P. Pantelides, H.E. Blomgren, D. Rammer. "Nonlinear models of multistory timber frames with timber buckling-restrained braces." Journal of Structural Engineering, (2024), 150(9): 04024106.

[13] American Plywood Association. "Freres mass ply panels (MPP), and mass ply lam (MPL) beams and columns." The Engineered Wood association, (2022), Rep. No. PR-L325. Tacoma, WA.

[14] American Society of Civil Engineers. "Minimum Design Loads and Associated Criteria for Buildings and Other Structures." ASCE 7-16, (2016), Reston, VA.

[15] Pacific Earthquake Engineering Research Center. "NGA-West 2 database flat file." PEER, (2025), https://ngawest2.berkeley.ed/databases/.

[16] Seismosoft. "Seismomatch – A computer program for spectrum matching of earthquake records." (2022), https://www.seismosoft.com/seismomatch.

[17] Federal Emergency Management Agency. Hazus earthquake model technical manual. (2022), Washington, DC.

[18] J.W. van de Lindt, S. Pei, S.E. Pryor, H. Shimizu, H. Isoda. "Experimental seismic response of a full-scale six-story light-frame wood building." Journal of Structural Engineering, (2010), 136 (10): 1262-1272.

[19] S. Pei, J.W. van de Lindt, A.R. Barbosa, J.W. Berman, E. McDonnell, J.D. Dolan, H.E. Blomgren, R.B. Zimmerman, D. Huang, S. Wichman. "Experimental seismic response of a resilient 2-story mass-timber building with post-tensioned rocking walls." Journal of Structural Engineering, (2019), 145 (11): 04019120.

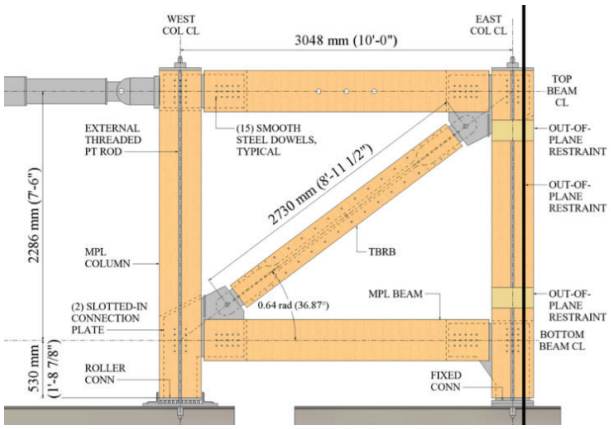

Figure 1. Experimental configuration of TBRB frame.

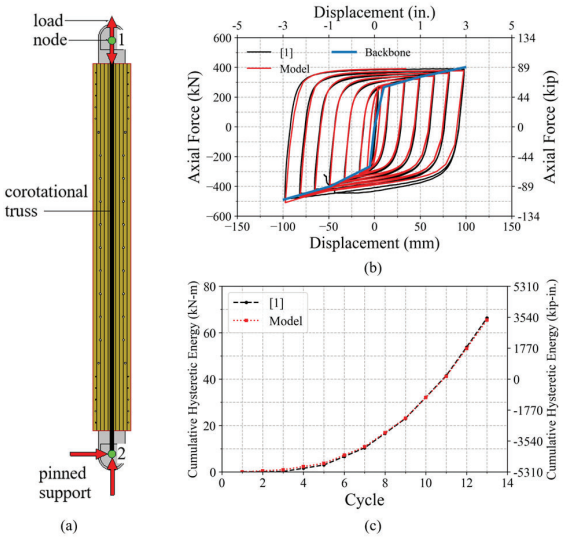

Figure 2. Numerical model of TBRB and comparison with experimental results: (a) component model; (b) hysteresis curves; and (c) cumulative hysteretic energy.

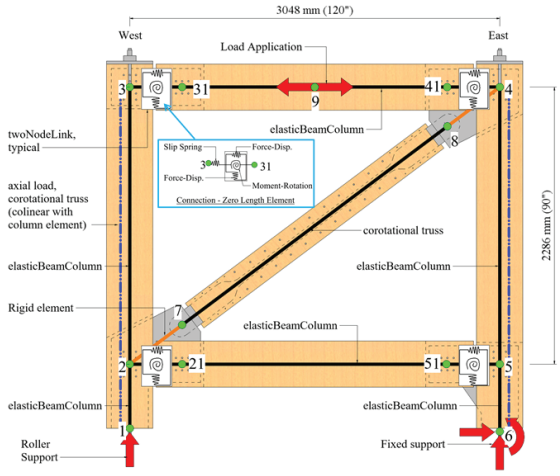

Figure 3. Numerical model schematic of single-story TBRB frame.

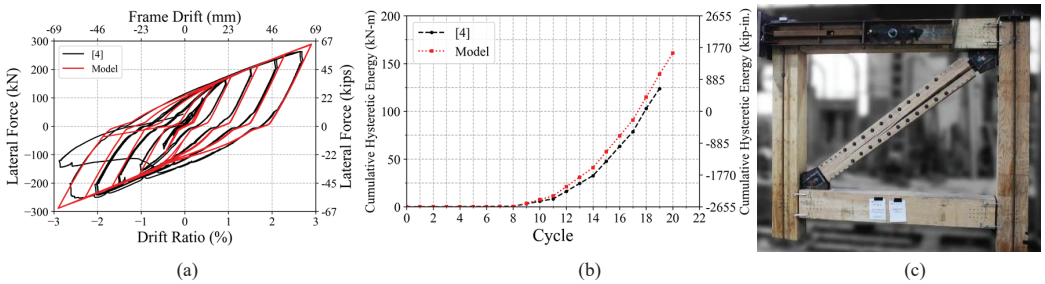

Figure 4. OpenSees single-story TBRBF model comparison with experiment I-BRB1 [4]: (a) test I-BRB1 hysteresis curve; (b) test I-BRB1 cumulative hysteretic energy; and (c) TBRB failure at the end of the experiment.

https://doi.org/10.52202/080513-0348

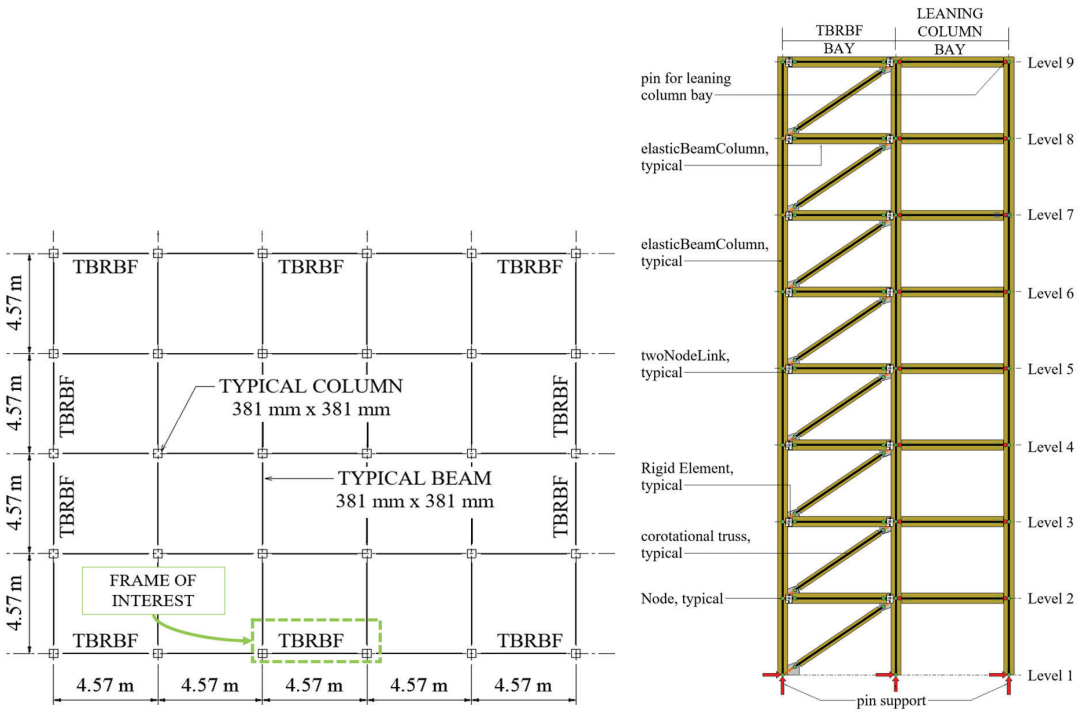

Figure 5. Eight-story building: (a) plan view of theoretical TBRB braced frame office building; (b) eight-story building TBRB braced frame model.

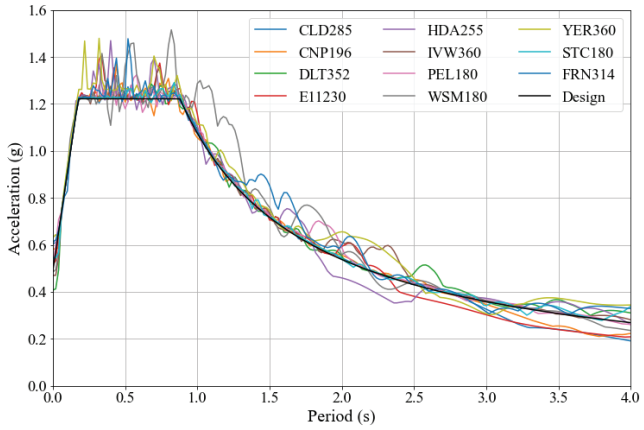

Figure 6. Eight-story building TBRB braced frame matched earthquake spectra for 10.0% probability of exceedance in 50 years.

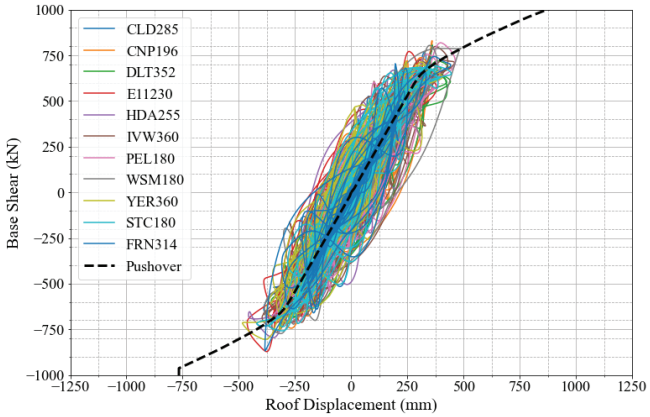

Figure 7. Eight-story TBRB braced frame base shear vs roof displacement results showing the static pushover and earthquake loading.

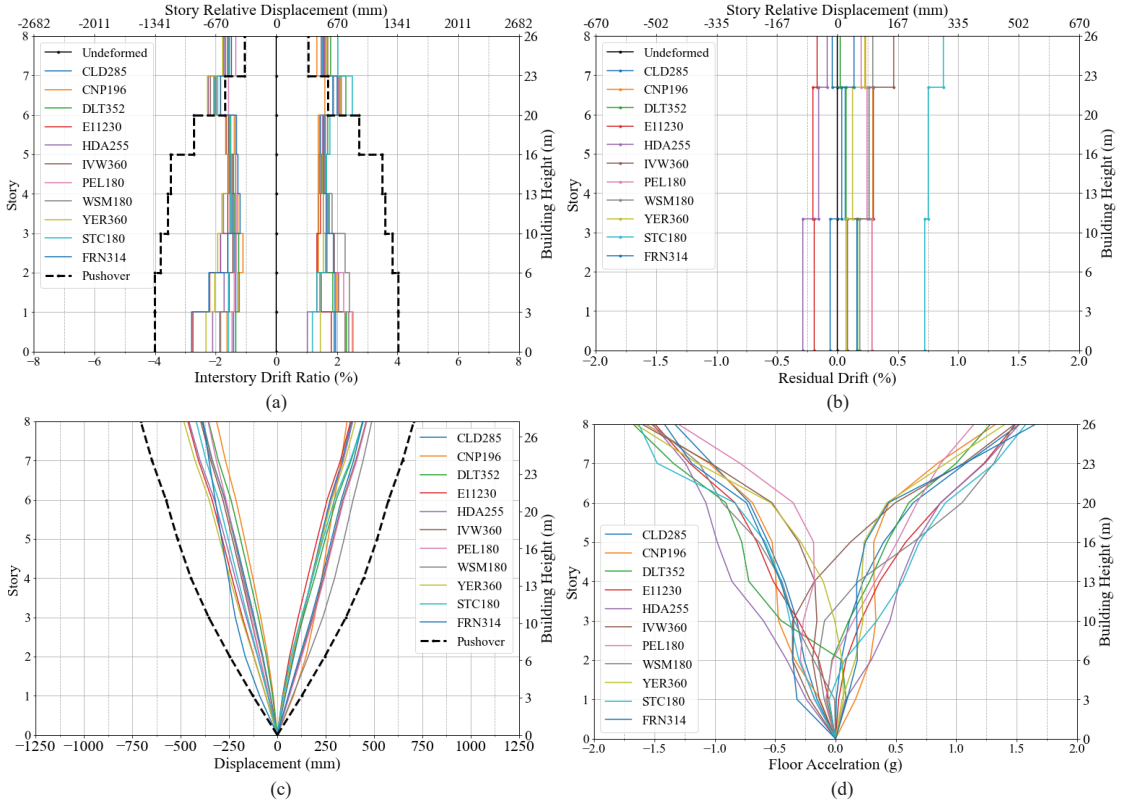

Figure 8. Eight-story building TBRB braced frame earthquake simulation: (a) peak story drifts; (b) residual story drifts; (c) building at peak roof displacement; and (d) peak floor accelerations.

https://doi.org/10.52202/080513-0348